Research Square

Preprints are preliminary reports that have not undergone peer review.
They should not be considered conclusive, used to inform clinical practice,
or referenced by the media as validated information.

# Rare-Earth-Element-Doped ZnO Thin Films for Gas Sensing and Solar-Cell Applications *A Critical Review of Structure–Property Relationships, Defect Chemistry, Surface Morphology and Device-Level Performance*

**C. S.A. Raj**

csaraj.aac@gmail.com

Arul Anandar College (Autonomous)

**Research Article**

**Keywords:** rare-earth doping, ZnO thin films, spray pyrolysis, gas sensors, ammonia, electron-transport layer, photovoltaic devices, X-ray diffraction, SEM, UV–visible spectroscopy, Tauc analysis, defect chemistry

**Posted Date:** October 26th, 2026

**DOI:** https://doi.org/10.21203/rs.3.rs-11479403/v1

**License:** This work is licensed under a Creative Commons Attribution 4.0 International License.
Read Full License

**Additional Declarations:** The authors declare no competing interests.

# Abstract

Rare-earth-element (REE) modification provides a route to tune the structure, surface chemistry, optical response and carrier transport of zinc oxide (ZnO), a wide-band-gap semiconductor used in resistive gas sensors and as a transparent or electron-transport layer in photovoltaic architectures. Yet the performance consequences of REE incorporation are strongly dependent on dopant identity, concentration, oxidation state, synthesis route, defect compensation and device architecture. This critical review examines how Ce, La, Nd, Sm, Eu, Gd, Tb, Dy, Er, Yb and related ions influence wurtzite phase stability, lattice strain, crystallite growth, surface morphology, optical absorption, Tauc-derived band-gap estimates, conductivity and interface behaviour. For gas sensing, the discussion connects adsorption and surface charge transfer to depletion-layer width, grain-boundary barriers, humidity dependence and selectivity. For photovoltaics, it distinguishes film-level optical/electrical indicators from complete-device metrics such as short-circuit current density, open-circuit voltage, fill factor, power-conversion efficiency and operational stability. Published examples include Nd-modified ZnO showing 43 s response and 12 s recovery to 25 ppm $NH_3$ at room temperature in a particular SILAR-prepared sensor, and recent Sm/Eu/Gd-doped samples with dopant-dependent ammonia response [1, 2]. These values are not directly comparable without harmonized protocols. The review emphasizes evidence quality, the danger of assigning visible photoluminescence uniquely to oxygen vacancies, and the need to verify dopant location using complementary methods. A composition–process–structure–defect–property–function framework is proposed to guide reproducible materials development and to prevent the mistaken assumption that a formulation optimized for gas adsorption will also optimize photovoltaic charge extraction.


# Highlights

• Rare-earth effects are dopant-, concentration-, process- and application-specific.

• XRD peak shifts alone do not prove substitutional incorporation; complementary chemical analysis is required.

• Gas-sensing gains may arise from surface chemistry and depletion modulation, but humidity and protocol differences complicate comparison.

• A lower optical band gap is not sufficient evidence of improved photovoltaic efficiency.

• Published figures require licence/permission checks; conceptual plots in this manuscript are explicitly labelled as illustrative.

# 1. Introduction

ZnO is a direct-transition semiconductor with a typical room-temperature optical gap in the approximate 3.2–3.4 eV range, high exciton binding energy and a hexagonal wurtzite structure. Its transparency and

process compatibility make it relevant to transparent electronics, ultraviolet optoelectronics, gas sensors and photovoltaic interfaces. However, native defects, surface adsorbates, grain boundaries, interfacial traps and processing-dependent stoichiometry can dominate measured properties. These sensitivities make ZnO a useful platform for defect and dopant engineering, but also make cross-study comparison difficult.

Rare-earth ions are attractive because their ionic radii and valence states differ from those of $Zn^{2+}$ and because their incorporation can perturb local coordination, charge compensation, surface chemistry and electronic states. Depending on the preparation conditions, a dopant may occupy a Zn site, reside at an interstitial or grain-boundary site, segregate at the surface, or form a secondary phase. The consequences are not equivalent. A change in XRD peak position may indicate strain or altered lattice spacing, but cannot by itself establish the dopant site; elemental mapping confirms spatial presence, not necessarily crystallographic occupancy [3–6].

The two application areas considered here have overlapping material requirements but distinct optimization targets. Gas sensors benefit from accessible reactive sites and measurable resistance changes, whereas photovoltaic electron-transport layers generally require low parasitic absorption, suitable band alignment, rapid extraction and low recombination. A high density of surface or bulk defects may improve gas adsorption while simultaneously creating non-radiative pathways in a solar cell. Recent reviews of REE-doped ZnO for perovskite solar cells and of ZnO-based gas sensors support the need for application-specific evaluation rather than a universal “doping improves performance” narrative [7, 8].

## 1.1 Scope and review questions

This review addresses: (i) how REE incorporation and processing affect ZnO phase, lattice parameters, crystallite size and morphology; (ii) how UV–visible absorption, transmittance, photoluminescence and Tauc-derived gaps should be interpreted; (iii) how electrical transport and grain boundaries interact with gas response; (iv) what evidence is required to establish benefits in photovoltaic devices; and (v) how future studies can report comparable, reproducible results.

# 2. Literature approach and evidence grading

| Evidence class | Definition used here | Examples of appropriate wording |
|---|---|---|
| Direct experimental | A paper reports a measured structure, spectrum, electrical value, sensor response or device metric. | “The authors reported…” |
| Mechanistic support | Spectroscopy, microscopy, calculations or electrical analysis support a proposed mechanism. | “The data are consistent with…” |
| Interpretation/hypothesis | A plausible mechanism not uniquely established for that sample. | “May reflect…; further confirmation is needed.” |
| Illustrative figure | Original schematic or conceptual plot with no experimental dataset. | “Conceptual illustration; not measured data.” |

## 3. Deposition routes and spray pyrolysis

ZnO:REE films have been fabricated using spray pyrolysis, chemical bath deposition, SILAR, sol–gel, sputtering, drop-casting and other methods. The method affects film thickness, porosity, substrate contact, grain-boundary density and defect populations. Spray pyrolysis is especially relevant to scalable coatings because precursor droplets are transported to a heated substrate, where solvent evaporation and precursor decomposition form the film. Deposition temperature, precursor molarity, solvent composition, spray rate, nozzle-to-substrate distance, carrier-gas flow, substrate temperature uniformity and post-annealing all influence the resulting material. Published studies have demonstrated REE-modified ZnO films made by chemical spray pyrolysis, including Nd/Tb co-doped films and Y-doped films [9, 10].

## 3.1 Process variables that must be reported

| Variable | Why it matters | Minimum reporting recommendation |
|---|---|---|
| Precursor chemistry | Controls decomposition, residual species and stoichiometry. | Chemical formula, purity, solvent, concentration and ageing time. |
| Substrate temperature | Controls droplet drying, reaction kinetics, grain growth and adhesion. | Measured surface temperature and tolerance, not only heater set point. |
| Spray conditions | Influence wetting, thickness uniformity and porosity. | Flow rate, nozzle type, distance, pulse/continuous mode and carrier gas. |
| REE concentration | May change defects, phase stability and grain growth non-monotonically. | Report nominal and measured dopant fraction with units and method. |
| Annealing | Can change oxygen stoichiometry, phase segregation and grain boundaries. | Atmosphere, temperature, duration, ramp and cooling conditions. |
| Film thickness | Affects transmission, sheet resistance and gas diffusion. | Profilometry/ellipsometry/cross-sectional SEM and uncertainty. |

# 4. Structural properties: phase, lattice and crystallite growth

X-ray diffraction (XRD) is commonly used to identify the wurtzite ZnO phase, preferred orientation, crystallite-size trends and possible secondary phases. The characteristic reflections often include the (100), (002) and (101) planes, with exact positions depending on instrument calibration, strain, composition and measurement conditions. Peak broadening may arise from finite coherent-domain size, microstrain, defects, instrumental broadening or overlapping reflections. Scherrer estimates should therefore be reported as apparent crystallite sizes unless instrumental broadening and strain contributions are treated appropriately.

The common Scherrer relation is $D = K\lambda/(\beta \cos \theta)$, where D is the apparent coherent-domain size, K is a shape factor, λ is the X-ray wavelength, β is the instrument-corrected full width at half maximum in radians and θ is the Bragg angle. Williamson–Hall or Rietveld methods may help separate size and strain contributions when the data quality supports them. A peak shift should not be assigned automatically to substitutional REE incorporation: stress, oxygen non-stoichiometry, sample displacement and phase mixtures can produce similar effects.

Experimental literature illustrates the importance of process-specific interpretation. Nd/Tb co-doped ZnO thin films prepared by chemical spray pyrolysis retained the wurtzite phase and showed changes in optical and electrical characteristics with dopant composition [9]. Y-doped films deposited by spray pyrolysis have also been investigated through XRD, FESEM and optical spectroscopy [10]. In a separate SILAR study, Kasirajan et al. examined Gd-, Nd- and Sm-modified ZnO films and related the structural/morphological data to room-temperature ammonia sensing [1]. Because the preparation routes differ, the reported trends should not be collapsed into one universal concentration law.

## 4.1 Secondary phases and dopant-site evidence

The absence of a separate REE-containing diffraction peak does not prove that every dopant ion is incorporated substitutionally; a low concentration, amorphous phase or nanoscale segregation may fall below the XRD detection limit. A defensible assignment combines XRD with XPS chemical-state analysis, STEM-EDS/EELS or carefully interpreted elemental mapping, Raman spectroscopy, and—where feasible—X-ray absorption or atom-probe methods. Surface-sensitive XPS should not be treated as a bulk-composition measurement, and EDS elemental detection alone does not resolve oxidation state or crystallographic site.

# 5. Surface morphology and microstructure

SEM and FESEM provide information on grain shape, agglomeration, porosity, cracks, coverage and pinholes. These features affect gas transport and accessible surface area, but they also influence electrical percolation and photovoltaic interface quality. For sensors, a porous surface can expose more adsorption sites; however, highly discontinuous or mechanically weak films may drift during cycling. For solar cells, dense, pinhole-free layers and reproducible contact with the absorber may be more valuable than maximum surface area.

Morphology comparisons require consistent magnification, scale bars, image acquisition conditions and sampling strategy. A single attractive micrograph cannot establish representative roughness or grain-size distribution. Quantitative image analysis should state the number of grains or fields measured, segmentation approach and uncertainty. If nanoparticle morphology is discussed alongside thin films, the distinction should remain explicit because particle powder images cannot substitute for film-surface or cross-sectional characterization.

# 6. Optical absorption, transmittance and band-gap analysis

UV–visible spectroscopy is often used to estimate absorption edges and visible-range transparency. For a thin film, absorbance depends on thickness, reflection, scattering and substrate baseline as well as absorption coefficient. If transmission and reflection are available, an absorption coefficient can be estimated with a model appropriate to the sample geometry; using absorbance alone without accounting for thickness may make comparisons unreliable.

For a direct allowed transition, the conventional Tauc form is $(\alpha h\nu)^2 = A(h\nu - E_g)$, where $\alpha$ is the absorption coefficient, $h\nu$ is photon energy, $A$ is a proportionality constant and $E_g$ is the estimated optical gap. The linear fitting interval must be justified and consistent. Defect-tail absorption, scattering, thickness variations, interference fringes and carrier-density effects can distort the intercept. The resulting $E_g$ is an optical estimate, not necessarily a direct measurement of the fundamental electronic band gap.

In the uploaded source manuscript, the reproduced figure from Dhiman et al. was accompanied by reported Tauc-derived values of 2.68 eV for ZnO, 2.59 eV for Sm-doped ZnO, 2.80 eV for Nd-doped ZnO and 2.47 eV for Dy-doped ZnO [11]. These values are specific to that nanoparticle study and should not be presented as universal thin-film values. Other REE-doped ZnO studies report gaps closer to the conventional ZnO range; for example, Tb-doped ZnO in a co-authored 2024 study was reported at 3.20 eV compared with 3.27 eV for the undoped material [12]. Such differences may reflect sample type, synthesis route, spectral processing and defect chemistry rather than an inconsistency that can be resolved by selecting a preferred number.

## 6.1 Interpreting optical shifts critically

A lower Tauc intercept can arise from disorder, defect-related absorption, band-tail states or true changes in electronic structure. A higher intercept may reflect carrier-concentration effects, altered crystallinity, or a different fitting window. Neither direction is intrinsically “better.” In a transparent electron-transport layer, strong visible absorption can be undesirable if it competes with the active absorber. Conversely, spectral conversion or defect-mediated absorption can be useful only if the generated carriers are collected rather than lost through non-radiative recombination.

## 6.2 Photoluminescence and defect assignments

Near-band-edge ultraviolet emission and broad visible emission are often discussed in terms of excitonic recombination and defects. However, visible bands should not be assigned uniquely to oxygen vacancies based on wavelength alone. Zinc interstitials, zinc vacancies, oxygen-related defects, surface states, impurities and defect complexes can produce overlapping features. Reliable assignments require corroboration using XPS, EPR, controlled-atmosphere annealing, temperature-dependent PL or other defect-sensitive measurements. An increased PL intensity is also ambiguous: it can indicate more radiative recombination or a change in absorption and optical outcoupling, not necessarily lower non-radiative loss.

# 7. Electrical properties and charge transport

Four-point-probe measurements provide sheet resistance; bulk resistivity requires reliable film thickness and geometric assumptions. Hall measurements can separate carrier concentration and mobility when the film is sufficiently conductive and contact quality is adequate. Impedance spectroscopy can help distinguish grain and grain-boundary responses, but equivalent-circuit models are often non-unique and should be supported by physical reasoning. Temperature-dependent conductivity can reveal activation energies, although the extracted value may represent grain-boundary barriers or multiple transport channels rather than one unique defect level.

| Measurement | Primary output | Common interpretation risk |
|---|---|---|
| Four-point probe | Sheet resistance; resistivity with thickness | Thickness uncertainty propagates into resistivity. |
| Hall effect | Carrier concentration and mobility | Contacts, geometry and multichannel conduction affect results. |
| Temperature-dependent I–V/σ | Effective activation energy | Several transport mechanisms can overlap. |
| Impedance spectroscopy | Frequency-dependent resistance/capacitance | Equivalent circuits may be non-unique. |
| XPS / UPS | Chemical state and surface energy levels | Surface sensitivity; charging and fitting assumptions. |
| Time-resolved PL | Carrier lifetime dynamics | Requires suitable excitation, fitting model and controls. |

## 8. Gas-sensing applications

In a common n-type ZnO resistive sensor, oxygen adsorbs at the surface and captures electrons, creating an electron-depleted near-surface region. Exposure to a reducing gas can consume adsorbed oxygen species and return electrons to the conduction network, often lowering resistance. Oxidizing gases may instead withdraw electrons and increase resistance. The precise response depends on temperature, oxygen partial pressure, humidity, grain size, contact geometry, illumination and the dominant surface reaction.

REE modification can affect adsorption energy, surface basicity, defect populations, catalytic reaction pathways and grain-boundary barriers. These explanations are plausible but must be demonstrated for each composition. The gas response is commonly reported as a percentage or resistance ratio; because definitions vary (for example, Rair/Rgas versus (Rair−Rgas)/Rgas), response values should not be compared unless the formula and test conditions match.

# 8.1 Quantitative examples from identified studies

Kasirajan et al. reported that a 3 wt% Nd-modified ZnO sensor prepared by SILAR showed response and recovery times of 43 s and 12 s, respectively, for 25 ppm $NH_3$ at room temperature [1]. A 2026 study of Sm-, Eu- and Gd-doped ZnO reported a 50% ammonia response for its Gd-doped sample, with rise and fall times of 6.4 s and 9.8 s under the study's conditions [2]. These are useful examples but cannot be ranked directly because the sensor response definitions, film geometries, gas-delivery systems, humidity, baselines and recovery criteria may differ.

Other studies explore rare-earth-modified ZnO for $NO_2$, CO and $CH_4$ under UV illumination, and Dy-modified ZnO films for $NO_2$ sensing [13, 14]. Such reports emphasize that gas identity and operating regime can change which surface state is beneficial. Room-temperature sensing is especially attractive

for low-power systems, but it requires careful assessment of baseline drift, humidity, UV power if used, and recovery under realistic air conditions.

| Benchmark parameter | Minimum report | Why it matters |
|---|---|---|
| Target gas and concentration | Gas identity, ppm/ppb, dilution method | Enables comparison and detection-limit estimation. |
| Response definition | Equation and sign convention | Prevents invalid ranking of percentages. |
| Response/recovery | Threshold definition, time window and cycle count | Avoids cherry-picking the fastest transient. |
| Operating environment | Temperature, relative humidity, oxygen and flow | Adsorption and reaction rates are environment-sensitive. |
| Selectivity | Interferents at stated concentrations | A large response to one gas is not sufficient. |
| Stability/repeatability | Independent cycles, devices, drift duration | Indicates suitability beyond a single test. |

## 9. Solar-cell applications

ZnO can serve as a transparent conducting oxide, a nanostructured scaffold or an electron-transport layer depending on the device architecture. In perovskite solar cells, the electron-transport layer should extract electrons efficiently, block holes, maintain appropriate energy alignment and minimize interfacial recombination. Rare-earth modification may alter carrier density, mobility, surface hydroxylation, defect distribution, work function and stability. These potential benefits are device-specific: conductivity measured on a standalone film does not guarantee higher power-conversion efficiency.

A recent review of REE-doped ZnO in perovskite solar cells discusses electron mobility, stability, photocarrier recombination and spectral conversion [7]. A separate review of dopant engineering for ZnO electron-transport layers emphasizes that dopant selection and device architecture must be treated together [15]. For a strong comparison, studies should report the absorber composition, ETL thickness, device architecture, active area, scan direction and rate, illumination calibration, stabilized maximum-power-point tracking, hysteresis and device statistics.

# 9.1 Device-level metrics

The principal photovoltaic metrics are open-circuit voltage (Voc), short-circuit current density (Jsc), fill factor (FF) and power-conversion efficiency (PCE). Under calibrated illumination, PCE is derived from the maximum electrical output relative to incident optical power. A change in optical band gap or sheet resistance is only an intermediate material property. Device claims require statistically meaningful comparisons against a control device fabricated under the same conditions.

| Material observation | Potential benefit | Possible adverse consequence | Necessary device validation |
|---|---|---|---|
| Higher conductivity | Lower series resistance, faster extraction | May not improve interface selectivity | Hall/4-point probe plus J–V and impedance. |
| Modified band alignment | Improved electron selectivity | An extraction barrier may form | UPS/XPS, Kelvin probe and device measurements. |
| More defect-related absorption | Possible sub-gap response | Trap-assisted non-radiative recombination | PL lifetime, EQE and recombination analysis. |
| Smoother/denser morphology | Fewer pinholes, improved contact | Lower surface area may matter in other architectures | AFM/SEM and cross-sectional imaging. |
| Improved thermal/chemical stability | Potential longer device lifetime | Stability may be limited by absorber/interface | Controlled ageing and stabilized PCE tracking. |

# 10. Integrated comparison and research gaps

The literature supports a non-monotonic and dopant-specific model. A dopant may improve surface reactivity or modify the depletion region while simultaneously reducing mobility, creating secondary phases or introducing recombination centres. The optimum sensor composition may therefore differ from the optimum photovoltaic interlayer. A dual-function claim should be reserved for studies that demonstrate both functions independently using application-relevant testing.

### 10.1 Priority research needs

- Establish dopant incorporation and oxidation state using multiple complementary methods rather than XRD or EDS alone.
- Report nominal and measured dopant concentrations with units and uncertainty; distinguish at.%, wt.% and mol%.
- Use calibrated UV–visible measurements with substrate baselines and thickness-aware absorption analysis; state the Tauc exponent and fitting interval.
- Standardize gas-response definitions, humidity, flow, interferents, cycling and long-term drift.
- Test photovoltaic performance in complete devices with statistical replication, stabilized efficiency and operational ageing.
- Include uncertainty estimates, raw-data availability where possible, and reproducible processing parameters.
- Evaluate dopant cost, toxicity, supply constraints and scalability alongside laboratory performance.

# 11. Conclusions

Rare-earth-element modification is a versatile strategy for tuning ZnO structure, morphology, optical response and electrical transport. Published work demonstrates dopant-dependent changes in ammonia sensing and optical/electrical properties, and recent reviews identify potential roles for REE-modified ZnO in photovoltaic electron-transport layers. The available evidence does not support a universal rule that rare-earth doping improves all performance metrics. Structural retention does not prove substitutional incorporation; a Tauc-derived gap shift does not identify its mechanism; visible PL is not a unique fingerprint of oxygen vacancies; and film-level conductivity does not prove higher solar-cell efficiency.

The strongest route forward is a composition–process–structure–defect–property–function framework supported by reproducible characterization and application-level validation. Sensor studies should prioritize selectivity, humidity tolerance, repeatability and drift alongside sensitivity. Photovoltaic studies should demonstrate improvements in complete devices, with stabilized performance and ageing data. Finally, figures reproduced from published papers must meet licence and permission requirements, while conceptual figures must remain clearly labelled as illustrative.

## References


1. Kasirajan K, Bruno Chandrasekar L, Maheswari S, Karunakaran M, Shunmuga Sundaram P (2021) A comparative study of different rare-earth (Gd, Nd, and Sm) metals doped ZnO thin films and its room temperature ammonia gas sensor activity. Opt Mater 121:111554. https://doi.org/10.1016/j.optmat.2021.111554
2. Prakash B, Isaiarasu IV, Khan FS, Alshahrani T, Shkir M (2026) Noticeable enhancement of ammonia gas sensing performance of ZnO thin films through Sm, Eu and Gd doping. Radiat Phys Chem 240:113468. https://doi.org/10.1016/j.radphyschem.2025.113468
3. Rahman MH, Rahaman MZ, Chowdhury EH, Motalab M, Hossain AKMA (2022) Understanding the role of rare-earth metal doping on the electronic structure and optical characteristics of ZnO. Mol Syst Des Eng 7:1516. https://doi.org/10.1039/D2ME00093H
4. Nanostructured Ce$_x$Zn$_{1-x}$O thin films (2014) Influence of Ce doping on the structural, optical and electrical properties. J Alloys Compd 588:170–176. https://doi.org/10.1016/j.jallcom.2013.10.210
5. Sharma N, Choudhury SP (2024) Gas sensing using metal oxide semiconductor doped with rare earth elements: a review. Mater Sci Engineering: B 307:117505. https://doi.org/10.1016/j.mseb.2024.117505
6. İpek Y, Ayhan NK (2021) Rare Earth Element Doped ZnO Thin Films and Applications. Int J Pure Appl Sci 7(2) https://dergipark.org.tr/en/pub/ijpas/article/944792
7. Mokgolo PJ, Gumede TP, Ocaya RO, Malevu TD (2025) Enhancing perovskite solar cells with rare-earth metal doped zinc oxide: A review of electron mobility, stability, and photocarrier recombination. Int J Energy Res 4240199. https://doi.org/10.1155/er/4240199

8. Krishna KG, Umadevi G, Parne S, Pothukanuri N (2023) Zinc oxide based gas sensors and their derivatives: a critical review. J Mater Chem C 11:3906–3925. https://doi.org/10.1039/D2TC04690C
9. Influence of Rare Earth (2017) Nd and Tb) Co-Doping on ZnO Thin Films Properties, physica status solidi. https://doi.org/10.1002/pssc.201700169
10. Influence of yttrium doping on the (2019) structural, morphological and optical properties of nanostructured ZnO thin films grown by spray pyrolysis. Ceram Int 45:6842–6852. https://doi.org/10.1016/j.ceramint.2018.12.178
11. Dhiman P, Rana G, Kumar A, Dawi EA, Sharma G (2023) Rare Earth Doped ZnO Nanoparticles as Spintronics and Photo Catalyst for Degradation of Pollutants. Molecules 28(6):2838. https://doi.org/10.3390/molecules28062838
12. Sebastian S, Raj CSA, Diana P, Ganesh V, Awwad NS, Yahia IS, AlAbdulaal TH (2024) Rare earth elements terbium (Tb), erbium (Er), ytterbium (Yb) doped zinc oxide nanoparticles: Synthesis structural optical and gas sensing studies. Physica B 694:416384. https://doi.org/10.1016/j.physb.2024.416384
13. Sayago I, Santos JP, Sánchez-Vicente C (2022) The Effect of Rare Earths on the Response of Photo UV-Activate ZnO Gas Sensors. Sensors 22(21):8150. https://doi.org/10.3390/s22218150
14. Dysprosium Doped Zinc Oxide for $NO_2$ Gas Sensing, (2022) Sensors 22:5173. https://pmc.ncbi.nlm.nih.gov/articles/PMC9317177/
15. Zainal NA, Abidin et al (2023) Dopant engineering for ZnO electron transport layer towards efficient perovskite solar cells. RSC Adv 13:33797–33819. https://doi.org/10.1039/D3RA04823C
16. Sebastian S, Raj CSA, Jacob SSK, Diana P, Ganesh V (2024) Effect of different solvents on ZnO thin films for gas sensing application by nebulizer spray pyrolysis method. Appl Phys A 130:615. https://doi.org/10.1007/s00339-024-07759-2
17. Enhancing Optoelectronic Performance Through Rare-Earth-Doped ZnO (2025) Insights and Applications. Photonics 12(5):454. https://www.mdpi.com/2304-6732/12/5/454
18. Sarf F, Karaduman Er I, Yakar E, Acar S (2020) The role of rare-earth metal (Y, Ru and Cs)-doped ZnO thin films in $NH_3$ gas sensing performances at room temperature. J Mater Sci: Mater Electron 31:10084–10095. https://doi.org/10.1007/s10854-020-03554-w
19. Saravanan K, Seenuvasakumaran P, Jabena Begum N, Balaji R (2025) Synthesis and characterization of ZnO and Ce-doped ZnO thin films by simplified spray pyrolysis technique. Ceram Int 51:62074–62082. https://doi.org/10.1016/j.ceramint.2025.10.440
20. Aparna KT, Velusamy P, Ramesh Babu R (2017) Effect of Sm doping on the physical properties of ZnO thin films deposited by spray pyrolysis technique, AIP Conference Proceedings 1832 080085. https://doi.org/10.1063/1.4980545
21. Salim K, Azzaoui W (2023) Physical properties of spray pyrolysed ZnO thin films obtained from nitrate, acetate and chloride precursors: Comparative study for Solar Cell Applications. Revista Mexicana de Física 69:031002. https://doi.org/10.31349/RevMexFis.69.031002

22. Enhancement in the Transport and Optoelectrical Properties of Spray Coated ZnO Thin Films by Nd Dopant, (2023) Electron Mater Lett. https://doi.org/10.1007/s13391-022-00381-5
23. Kumar V et al (2017) Rare Earth Doped Zinc Oxide Nanophosphor Powder: A Future Material for Solid State Lighting and Solar Cells. ACS Photonics 4(11):2613–2637. https://doi.org/10.1021/acsphotonics.7b00777
24. Band Gap Engineering and Relationship with Luminescence in Rare-Earth Elements Doped ZnO: An Overview. Mater Technol (2022) https://doi.org/10.1080/10667857.2022.2082351
25. Rare earth element doping (2026) in ZnO nanostructures: A critical review of energy transfer, design, and optoelectronic applications. J Lumin 295:121863. https://doi.org/10.1016/j.jlumin.2026.121863
26. Defect-Driven (2026) Selectivity Inversion in ZnO Gas Sensors via $Y^{3+}$ and $Dy^{3+}$ Doping for Enhanced VOC Detection with a Suppressed $NO_2$ Response. Sensors 26:4675. https://doi.org/10.3390/s26154675
27. ZnO Thin Films Synthesized by Ultra Spray Pyrolysis (2026) Structural Characterization, Gas Sensing Behaviour and Antimicrobial Activity. Asian J Chem 38(2):425–433. https://doi.org/10.14233/ajchem.2026.34808
28. Optical (2015) Sensing Properties of Cu Doped ZnO Nanocrystalline Thin Films. J Nanatechnol 172864. https://doi.org/10.1155/2015/172864
29. Rare-earth (2026) element doping in ZnO nanostructures: a critical review of energy transfer, design, and optoelectronic applications. J Lumin. https://doi.org/10.1016/j.jlumin.2026.121863
30. Özgür Ü, Alivov YI, Liu C, Teke A, Reshchikov MA, Doğan S, Avrutin V, Cho S-J, Morkoç H (2005) A comprehensive review of ZnO materials and devices. J Appl Phys 98:041301. https://doi.org/10.1063/1.1992666
31. Janotti A, Van de Walle CG (2009) Fundamentals of zinc oxide as a semiconductor. Rep Prog Phys 72:126501. https://doi.org/10.1088/0034-4885/72/12/126501
32. Batzill A, Diebold U (2005) The surface and materials science of zinc oxide. Prog Surf Sci 79:47–154. https://doi.org/10.1016/j.progsurf.2005.07.002
33. Fortunato E, Barquinha P, Martins R (2012) Oxide semiconductor thin-film transistors: a review of recent advances. Adv Mater 24:2945–2986. https://doi.org/10.1002/adma.201103228
34. Tauc J, Grigorovici R, Vancu A (1966) Optical properties and electronic structure of amorphous germanium. Phys Status Solidi (b) 15:627–637. https://doi.org/10.1002/pssb.19660150224
35. Korotcenkov G (2007) Metal oxides for solid-state gas sensors: What determines our choice? Mater Sci Eng B 139:1–23. https://doi.org/10.1016/j.mseb.2007.01.044
36. Wang ZL (2004) Zinc oxide nanostructures: growth, properties and applications. J Phys: Condens Matter 16:R829–R858. https://doi.org/10.1088/0953-8984/16/25/R01
37. Klingshirn C (2007) ZnO: Material, physics and applications. ChemPhysChem 8:782–803. https://doi.org/10.1002/cphc.200700002

38. Look DC (2001) Recent advances in ZnO materials and devices. Mater Sci Eng B 80:383–387. https://doi.org/10.1016/S0921-5107(00)00604-6
39. Ellmer A (2012) Past achievements and future challenges in the development of optically transparent electrodes. Nat Photonics 6:809–817. https://doi.org/10.1038/nphoton.2012.282
40. Minami T (2005) Transparent conducting oxide semiconductors for transparent electrodes. Semicond Sci Technol 20:S35–S44. https://doi.org/10.1088/0268-1242/20/4/004
41. Pearton SJ, Norton DP, Ip K, Heo YW, Steiner T (2005) Recent progress in processing and properties of ZnO. Prog Mater Sci 50:293–340. https://doi.org/10.1016/j.pmatsci.2004.04.001
42. Sberveglieri C (1995) Recent developments in semiconducting thin-film gas sensors. Sens Actuators B 23:103–109
43. Barsan N, Koziej D, Weimar U (2007) Metal oxide-based gas sensor research: How to? Sens Actuators B 121:18–35. https://doi.org/10.1016/j.snb.2006.09.047
44. Yamazoe N (2005) Toward innovations of gas sensor technology. Sens Actuators B 108:2–14. https://doi.org/10.1016/j.snb.2004.12.075
45. Wang C, Yin L, Zhang L, Xiang D, Gao R Metal oxide gas sensors: Sensitivity and influencing factors. Sensors 10 (2010) 2088–2106. https://doi.org/10.3390/s100302088
46. Dey A (2018) Semiconductor metal oxide gas sensors: A review. Mater Sci Eng B 229:206–217. https://doi.org/10.1016/j.mseb.2017.12.036
47. Comini E (2006) Metal oxide nano-crystals for gas sensing. Anal Chim Acta 568:28–40. https://doi.org/10.1016/j.aca.2005.10.064
48. Korotcenkov G (2007) Metal oxides for solid-state gas sensors: What determines our choice? Mater Sci Eng B 139:1–23. https://doi.org/10.1016/j.mseb.2007.01.044
49. Seiyama T, Kato A, Fujita K, Nagatani M (1962) A new detector for gaseous components using semiconductive thin films. Anal Chem 34:1502–1503. https://doi.org/10.1021/ac60191a001
50. Morkoç M, Özgür Ü (2009) Zinc Oxide: Fundamentals, Materials and Device Technology. Wiley-VCH, Weinheim. https://doi.org/10.1002/9783527623945
51. Janotti A, Van de Walle CG (2007) Native point defects in ZnO. Phys Rev B 76:165202. https://doi.org/10.1103/PhysRevB.76.165202
52. Janotti A, Van de Walle CG (2005) Oxygen vacancies in ZnO. Appl Phys Lett 87:122102. https://doi.org/10.1063/1.205336
53. Limpijumnong S, Zhang SB, Wei SH, Park CH (2004) Doping by group-I elements in ZnO. Phys Rev Lett 92:155504. https://doi.org/10.1103/PhysRevLett.92.155504
54. Tsukazaki A et al (2005) Repeated temperature modulation epitaxy for p-type doping and light-emitting diode based on ZnO. Nat Mater 4:42–46. https://doi.org/10.1038/nmat1274
55. Mass J, Bhardwaj P, Kundu J (1997) Spray deposition of zinc oxide thin films. Sol Energy Mater Sol Cells 45:1–12

56. Ayouchi R, Leinen D, Martín F, Gabás M, Dalchiele E, Ramos-Barrado JR (2003) Preparation and characterization of transparent ZnO thin films obtained by spray pyrolysis. Thin Solid Films 426:68–77. https://doi.org/10.1016/S0040-6090(02)01232-9
57. Perednis D, Gauckler LJ (2005) Thin film deposition using spray pyrolysis. J Electroceram 14:103–111. https://doi.org/10.1007/s10832-005-0870-x
58. Fortunato E, Ginley D, Hosono H, Paine DC (2007) Transparent conducting oxides for photovoltaics. MRS Bull 32:242–247. https://doi.org/10.1557/mrs2007.29
59. Gümüş C, Özkendir OM, Kavak H, Ufuktepe Y (2006) Structural and optical properties of zinc oxide thin films prepared by spray pyrolysis method. J Optoelectron Adv Mater 8:299–303
60. Major S, Banerjee A, Chopra KL (1983) Highly transparent and conducting indium-doped zinc oxide films by spray pyrolysis. Thin Solid Films 108:333–340
61. Singh AK, Janotti A, Scheffler M, Van de Walle CG (2008) Sources of electrical conductivity in ZnO. Phys Rev Lett 101:055502. https://doi.org/10.1103/PhysRevLett.101.055502
62. Chen JT, Wang J, Zhang F, Zhang GA, Wu ZG, Yan PX (2008) The effect of substrate temperature on the structural and optical properties of ZnO films prepared by spray pyrolysis. J Cryst Growth 310:2627–2632
63. Uday Balegar S, Srinatha N, Shashidhar R, Raghu A (2023) Annealing temperature-dependent structural and optical characteristics of spray pyrolyzed ZnO thin films, Materials Today: Proceedings 92 1453–1458. https://doi.org/10.1016/j.matpr.2023.05.651
64. Srivathsa M, Rajendra BV (2022) A study on structure, surface morphology, optical and electrical properties of spray pyrolyzed ZnO and Zn0.97Nd0.03O thin films, Materials Today: Proceedings 55 87–93. https://doi.org/10.1016/j.matpr.2021.12.302
65. Study the (2024) characterization of ZnO and AZO films prepared by spray pyrolysis and the effect of annealing temperature. Opt Mater 150:115261. https://doi.org/10.1016/j.optmat.2024.115261
66. Influence of Annealing on Properties of Spray Deposited ZnO Thin Films J Nanomaterials (2013) Article 146382. https://doi.org/10.1155/2013/146382
67. Liu C, Xiao C, Li W (2021) Zinc oxide nanoparticles as electron transporting interlayer in organic solar cells. J Mater Chem C 9:14093–14114. https://doi.org/10.1039/D1TC03434K
68. Han Y et al (2023) Solution-Processable Zinc Oxide for Printed Photovoltaics: Progress, Challenges, and Prospect. Adv Energy Sustain Res 4:2200179. https://doi.org/10.1002/aesr.202200179
69. Zhang P et al (2018) Perovskite Solar Cells with ZnO Electron-Transporting Materials. Adv Mater 30:1703737. https://doi.org/10.1002/adma.201703737
70. Qiu C, Wu Y, Song J, Wang W, Li Z (2022) Efficient Planar Perovskite Solar Cells with ZnO Electron Transport Layer, Coatings 12 1981. https://doi.org/10.3390/coatings12121981
71. Zainal NA, Abidin et al (2023) Dopant engineering for ZnO electron transport layer towards efficient perovskite solar cells. RSC Adv 13:33797–33819. https://doi.org/10.1039/D3RA04823C

72. Gantumur M et al (2024) Tungsten-Doped ZnO as an Electron Transport Layer for Perovskite Solar Cells: Enhancing Efficiency and Stability. ACS Appl Mater Interfaces 16:36255–36271. https://doi.org/10.1021/acsami.4c03591
73. Consonni V, Briscoe J, Kärber E, Li X, Cossuet T (2019) ZnO nanowires for solar cells: a comprehensive review. Nanotechnology 30:362001. https://doi.org/10.1088/1361-6528/ab1f2e
74. Manser JS, Christians JA, Kamat PV (2016) Intriguing optoelectronic properties of metal halide perovskites. Chem Rev 116:12956–13008. https://doi.org/10.1021/acs.chemrev.6b00136
75. Grätzel M (2003) Dye-sensitized solar cells. J Photochem Photobiol C 4:145–153. https://doi.org/10.1016/S1389-5567(03)00026-1
76. O'Regan B, Grätzel M (1991) A low-cost, high-efficiency solar cell based on dye-sensitized colloidal TiO2 films. Nature 353:737–740. https://doi.org/10.1038/353737a0
77. Green MA (1981) Solar cell fill factors: General graph and empirical expressions. Solid State Electron 24:788–789. https://doi.org/10.1016/0038-1101(81)90062-9
78. Nelson J (2003) The Physics of Solar Cells. Imperial College, London. https://doi.org/10.1142/p276
79. Devadiga D, Selvakumar M, Shetty P, Santosh MS (2021) Recent progress in solar cells based on zinc oxide nanostructures. J Power Sources 493:229698. https://doi.org/10.1016/j.jpowsour.2021.229698
80. Toma FTZ, Rahman MS, Maria KH (2025) A review of recent advances in ZnO nanostructured thin films by various deposition techniques. Discover Mater 5 Article 60. https://doi.org/10.1007/s43939-025-00201-1
81. Zinc Oxide Nanostructures in Photovoltaics (2026) Recent Progress, Technical Challenges and Perspectives. Chemistry—An Asian J 26:e2500142. https://doi.org/10.1002/tcr.202500142

# Figures

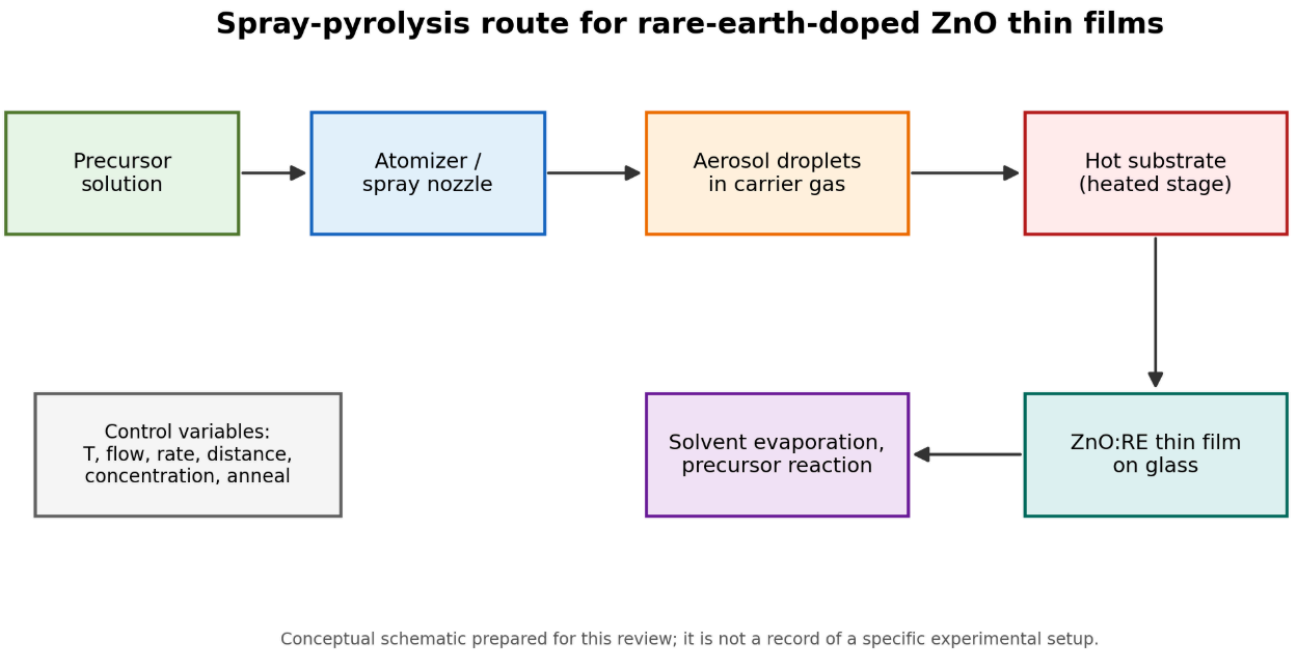



**Figure 1**

*Conceptual spray-pyrolysis workflow for ZnO:REE films. Original schematic prepared for this review; it does not represent a specific apparatus or experimental parameter set.*




**Figure 2**

*Illustrative XRD envelope showing the concept of small diffraction changes in a doped material. This is a schematic generated for explanation—not measured or digitized experimental data—and must not be used to extract lattice constants or crystallite sizes.*

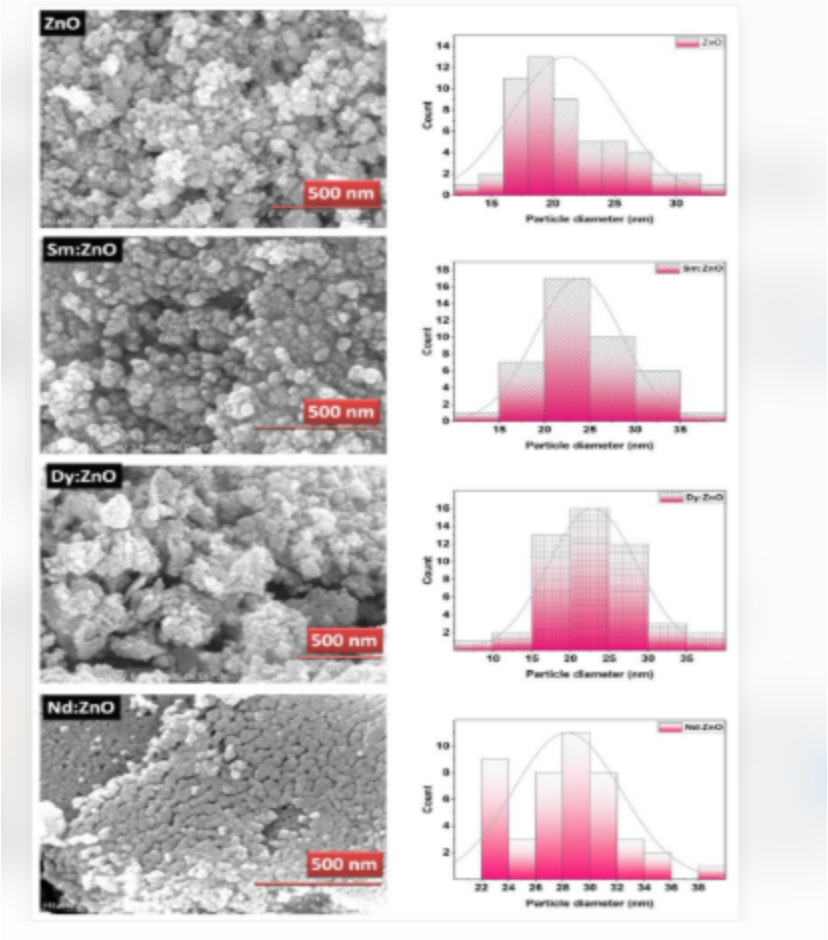



**Figure 3**

*Published SEM micrographs and particle-size distributions for ZnO and selected REE-doped ZnO nanoparticle samples, as included in the source manuscript. Source: Dhiman et al. (2023) [11]. These are nanoparticle images, not spray-pyrolysed thin-film cross-sections. Reproduction permission/licence compatibility must be checked before submission.*

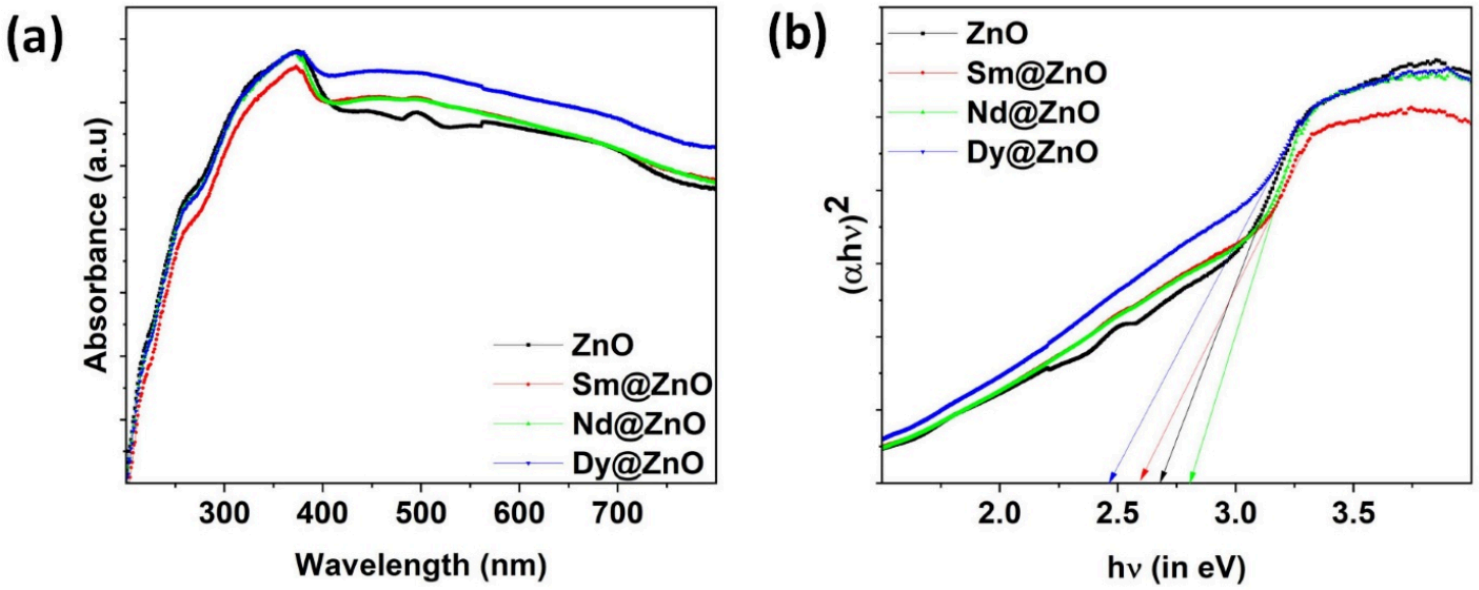



**Figure 4**

*Published UV–visible absorbance and Tauc-style plots for ZnO and Sm-, Nd- and Dy-modified ZnO, as embedded in the supplied manuscript. Source: Dhiman et al. (2023) [11]. Values are specific to that published nanoparticle study.*

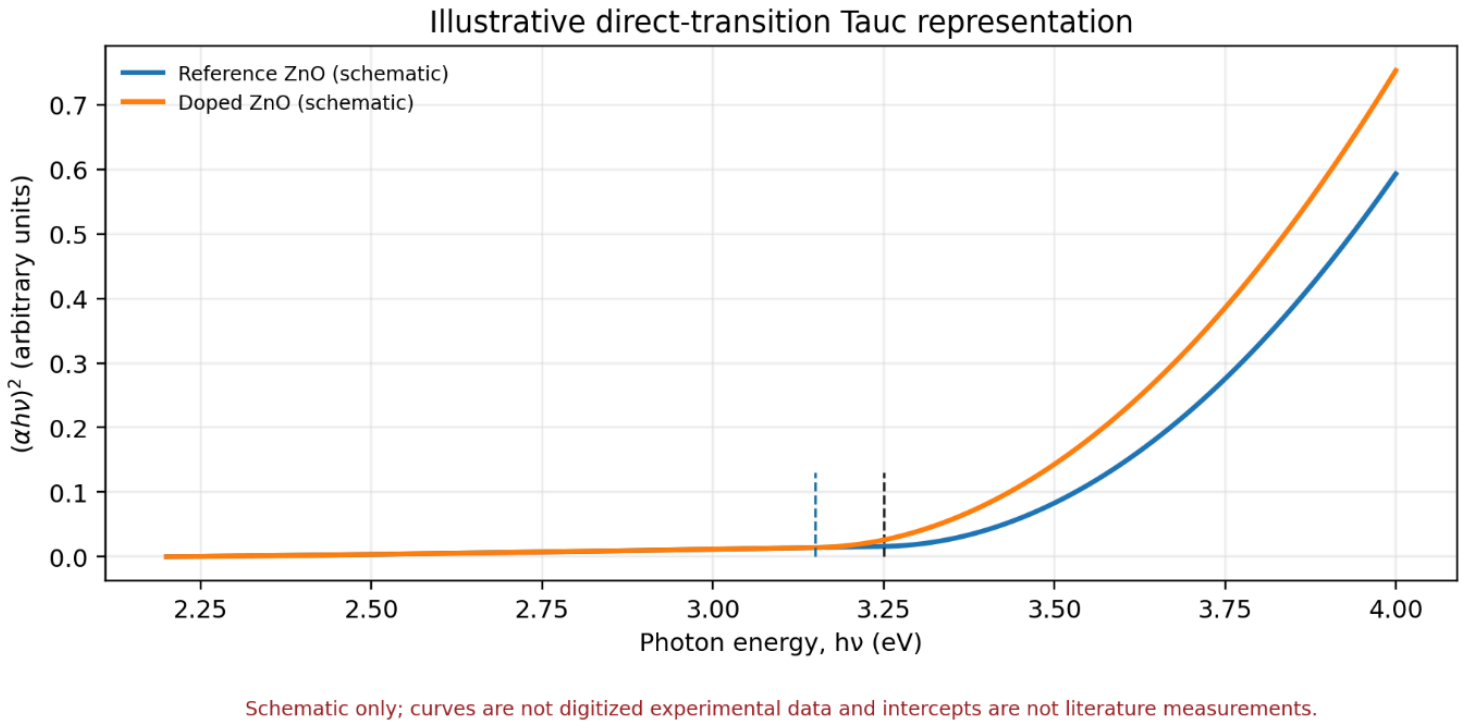
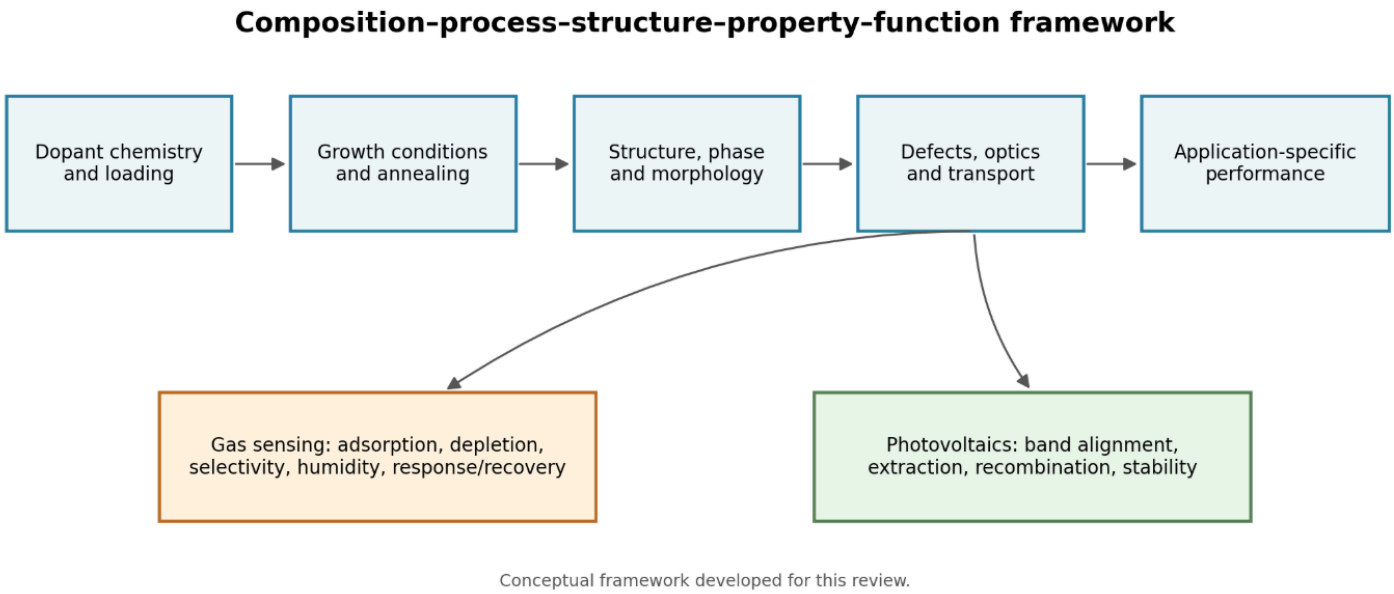



**Figure 5**

*Conceptual direct-transition Tauc plot. Curves are simulated solely to explain the extrapolation method; they are not experimental data and must not be used as evidence for a numerical band-gap shift.*




## Figure 6

*Composition–process–structure–property–function framework proposed in this review. Original conceptual figure; it is not a fitted or validated predictive model.*